

Digital Beamforming in Ultrasound Imaging

Sverre Holm

Vingmed Sound AS, Research Department, Vollsveien 13C, N-1324 Lysaker, Norway,
Department of Informatics, University of Oslo, Norway

ABSTRACT

In medical ultrasound imaging, beam control methods such as dynamic focusing, and dynamic aperture and weighting give a need for more flexible control over the receive beam. In addition the desire to increase acquired framerate makes it a requirement to be able to receive several beams in parallel for each transmitted beam. Digital beamforming implemented with custom VLSI chips will give these capabilities. This paper therefore discusses various concepts for digital beamforming and also gives a discussion of the effect of time delay quantization in beamforming under conditions of steering and focusing.

1. INTRODUCTION

Beamforming in ultrasound instruments for medical imaging has traditionally been implemented using analog delay lines. Typically arrays with between 48 and 128 elements are used. The signal from each individual element is to be delayed in order to steer the beam in the desired direction. This is similar to beamforming in sonar and radar systems. In addition ultrasound systems need to focus the beam also. In the receive beamformer this gives rise to the concept of dynamic focusing. For each pulse which is transmitted from the array, the receive beamformer tracks the depth and focuses the receive beam as the depth increases. It is often also desirable to let the receive aperture increase with depth. This gives a lateral resolution which is constant with depth, and decreases the sensitivity to aberrations in the imaged medium in the nearfield. This gives a requirement for dynamic control of the number of elements that are used. Since often a weighting function (apodization) is used for sidelobe reduction, the element weights also have to be dynamically updated with depth.

Digital beamforming is now about to become feasible in such beamformers. The concept has long been known, but availability of high-speed analog to digital converters, and VLSI technology improvements have

now made digital beamformers feasible. Some work in this area has been reported in [1] and [2]. In addition to obtaining a more accurate realization of a beamformer, digital beamforming also opens up for new possibilities such as several parallel receive beams [3] which give an increased frame rate.

The purpose of this paper is first to review the basic principles for beamforming by discussing direct time-delay beamforming, and complex or real down-mixing. The down-mixing schemes require lower sample rates than the direct implementation if the signal's bandwidth is restricted. Second the effects of quantization of the time delays in a digital beamformer are considered.

2. BEAMFORMER CONCEPTS

2.1 Baseband Beamforming

This concept is a straightforward implementation of time-delay beamforming, i.e. the output is:

$$h(t) = \sum_{m=0}^{M-1} w_m x_m(t - \tau_m) \quad (1)$$

where x_m is the output from each array element, τ_m is the desired dynamically updated delay, and w_m is the dynamically updated weighting. The requirements for time delay accuracy in this scheme are very high as later analysis will show. This can be overcome in two different ways:

1. Interpolation.

In this scheme a relatively low sample rate determined by the maximum frequency is used and then the data is interpolated up to the required accuracy [4]. Typical interpolation factors are two, four and eight. The group delay and frequency response characteristics of the interpolator determine quality.

2. Course delay and vernier phase shifter.

In this scheme course delays with accuracy given by the sample rate and maximum frequency are followed by a vernier control which is implemented by a phase shifter tuned to midband. The phase shifter is an approximation to a time delay and is

exact only at the center frequency. An analysis of the error is given in [5].

2.2 Down-Mixing

An alternative for processing an input of limited bandwidth is to mix down to an intermediate frequency (shifted sideband beamforming) or baseband. The down-mixing can be done digitally after sampling [1] or in the analog domain [2] prior to sampling. In addition the down-mixing can be done using a complex or a real mixer.

1. Complex Down-Mixing

Complex down-mixing can be formulated by shifting the complex input signal in each channel by $-\omega_0$:

$$\begin{aligned} h(t) &= \sum_{m=0}^{M-1} w_m x_m(t - \tau_m) e^{-j\omega_0(t - \tau_m)} \\ &= e^{-j\omega_0 t} \sum_{m=0}^{M-1} w_m x_m(t - \tau_m) e^{j\omega_0 \tau_m} \end{aligned} \quad (2)$$

Thus it is seen that there is an extra phase factor in each channel which depends on the delay. This factor must be removed by a complex multiplication with $e^{-j\omega_0 \tau_m}$ in each channel. Compared to time delay beamforming, the required phase accuracy is given by the center frequency, while the required delay accuracy is determined by the much smaller bandwidth. This is the advantage of this scheme.

In medical imaging, typically transducers have had a bandwidth in the order of 40-50% of the center frequency. Therefore there is a potential for a saving by a factor of two in the sample rate using this scheme. As transducers tend towards relative bandwidths up to 80%, the saving in sample rate disappears. Other disadvantages are the need for a complex mixer and delays, and a phase multiplier in each channel prior to the beamformer.

2. Real Down-mixing

A real input signal can be expressed by the complex envelope:

$$y(t) = 2\text{Re}(x(t)e^{j\omega_0 t}) = x(t)e^{j\omega_0 t} + x^*(t)e^{-j\omega_0 t} \quad (3)$$

For this signal the beamformed output should be:

$$\begin{aligned} h(t) &= \sum_{m=0}^{M-1} 2\text{Re}(x_m(t - \tau_m)e^{j\omega_0(t - \tau_m)}) \\ &= \sum_{m=0}^{M-1} x_m(t - \tau_m)e^{j\omega_0(t - \tau_m)} + x_m^*(t - \tau_m)e^{-j\omega_0(t - \tau_m)} \end{aligned} \quad (4)$$

In order to avoid the complex delays, real down-mixing can be used. Assume that each channel is moved down to an intermediate frequency by mixing with $2\cos\omega_1 t = e^{j\omega_1 t} + e^{-j\omega_1 t}$, and then delayed.

The beamformer output after filtering out the components at $\pm(\omega_0 + \omega_1)$ is:

$$\begin{aligned} h'(t) & \\ &= \sum_{m=0}^{M-1} x_m(t - \tau_m)e^{j(\omega_0 - \omega_1)(t - \tau_m)} + x_m^*(t - \tau_m)e^{-j(\omega_0 - \omega_1)(t - \tau_m)} \end{aligned} \quad (5)$$

This is equivalent to:

$$h'(t) = (1/2) \sum_{m=0}^{M-1} \text{Re}(x_m(t - \tau_m)e^{j(\omega_0 - \omega_1)(t - \tau_m)}) \quad (6)$$

Compared to (4), in addition to a change of center frequency, an extra phase factor of $e^{j\omega_1 \tau_m}$ has been added and needs to be compensated for. This phase factor can be included in the mixer for each channel and be dynamically updated. The advantage over the complex mixer scheme is that only one delay line per channel is required.

3. TOLERANCE ANALYSIS

An array may deviate from the ideal characteristics in the form of a phase aberration, or in element gain. It turns out that the most critical one is a deviation in phase, as for instance caused by quantization effects in the time delays or offsets in the element locations. The time delays are determined by the steering and focusing, and the distribution of the phase error over the array may be divided into the following cases:

1. Random phase errors are assumed to be uncorrelated from element to element and give rise to a sidelobe structure which is also random as a function of angle and which can be characterized by a mean sidelobe level.
2. Focusing with a quantized quadratic time delay function gives rise to discrete sidelobes near the main lobe.
3. Periodic errors occur in unfocused uniform arrays (i.e. with uniform distance between individual elements) when steered to certain directions and give rise to strong discrete sidelobes.
4. Steering in combination with focusing gives discrete quantization sidelobes that often are higher than those caused by focusing alone. They are therefore of importance since they determine the worst-case sidelobe level in a focused imaging system.

All four cases will be discussed for the direct time-delay beamformer.

3.1 Model

The effect of time or phase errors can be found by considering the time delay, low-pass beamformer:

$$h(t, \theta, r) = \sum_{m=0}^{M-1} w_m x_m(t - \tau_m) \quad (7)$$

where $h(t, \theta, r)$ is the beamformer output, $x_m(t)$ is the input from element number m in an array with M elements, and w_m is the weighting or apodization. The time-delay for each element, τ_m , is determined by the direction, θ , that the array is steered to and in a focused system also the depth, r . When the beamformer is steered to a direction, θ off broadside in the far-field, the time delays are given by:

$$\tau_{m,steer} = ((m - M/2) d \sin \theta) / c \quad (8)$$

where d is the interelement distance and c the velocity of sound. If the beamformer is focused at the point (r, θ) , an additional focusing time delay is added:

$$\begin{aligned} \tau_{m,focus} &= [r - x \sin \theta - \sqrt{(r - x \sin \theta)^2 + d^2 (m - M/2)^2 \cos^2 \theta}] / c \\ &\approx - \frac{[(m - M/2) d \cos \theta]^2}{2rc} \end{aligned} \quad (9)$$

where the approximation is the Fresnel approximation. A narrowband signal will now be assumed and complex notation will be used in order to model the effect of errors in the down-mixed, baseband output from the beamformer. First, let the signal be a continuous sine-wave of frequency $\omega_0 = 2\pi f_0$, received from a point source at (θ^s, r^s) with source delay τ_m^s given by (8) and (9):

$$x_m(t|\theta^s, r^s) = \exp(j\omega_0(t + \tau_m^s)) \quad (10)$$

The beamformer delays found from (8) and (9) will be quantized to $\hat{\tau}_m = n/f_s$, where n is integer and f_s is the sampling frequency. The level of the sidelobes (whether random or discrete) is given by the number of quantization steps per period of the beamformed signal, M_q . The oversampling ratio is $M_q = f_s/f_0$ i.e. the ratio of the sampling frequency and the signal frequency. After quantization of the delay, there will be a phase error per element, e_m , in the range $[-\pi/M_q, \pi/M_q]$. Likewise the amplitude is assumed nominally to be unity, and to have an error a_m that varies from element to element.

The output of the beamformer can then be expressed as:

$$\begin{aligned} h(t, \theta, r|\theta^s, r^s) & \\ &= \sum_{m=0}^{M-1} w_m \cdot (1 + a_m) \cdot \exp(je_m) \cdot \exp(j\omega_0(t + \tau_m^s - \tau_m)) \end{aligned} \quad (11)$$

Thus the desired response is seen through a phase grating. The beam pattern is obtained as the time average and is:

$$\begin{aligned} & \sum_{m=0}^{M-1} w_m \cdot (1 + a_m) \cdot \cos e_m \cdot \exp(j\omega_0(t + \tau_m^s - \tau_m)) \\ & + j \sum_{m=0}^{M-1} w_m \cdot (1 + a_m) \cdot \sin e_m \cdot \exp(j\omega_0(\tau_m^s - \tau_m)) \end{aligned} \quad (12)$$

It is here separated in a slightly perturbed desired response and an additional undesired response. When the phase and amplitude errors are small, the trigonometric terms may be expanded in a power series, and an approximation may be obtained by retaining the first terms.

$$\begin{aligned} h(\theta, r|\theta^s, r^s) &\approx \sum_{m=0}^{M-1} w_m \cdot \exp(j\omega_0(\tau_m^s - \tau_m)) \\ & + j \sum_{m=0}^{M-1} w_m \cdot e_m \cdot \exp(j\omega_0(\tau_m^s - \tau_m)) \\ & + \sum_{m=0}^{M-1} w_m \cdot a_m \cdot \exp(j\omega_0(\tau_m^s - \tau_m)) \end{aligned} \quad (13)$$

Thus, in the far-field where $(\tau_m^s - \tau_m)$ varies linearly with m as given by (8), the beam pattern consists of the desired response and additive terms which are given by the Fourier transform of the time delay error and the amplitude error over the array. For a focused system, the Fourier transform generalizes to a focused delay sum with τ_m and τ_m^s given by the sum of (8) and (9), but the analysis of the effect of errors is essentially the same. The properties of the phase error in the two cases are however quite different as will be shown here.

The properties of the weighting function are important in the subsequent analysis and therefore some characteristics will be defined. The normalized Coherent Power Gain (CPG) and the normalized Incoherent Power Gain (IPG) are defined as:

$$\text{CPG} = \left[\frac{1}{M} \sum_{m=0}^{M-1} w_m \right]^2 \quad \text{IPG} = \frac{1}{M} \sum_{m=0}^{M-1} w_m^2 \quad (14)$$

The ratio of the two is in spectral analysis called the normalized Equivalent Noise Bandwidth (ENBW). In

the context of spatial processing a more suitable term is Equivalent Noise Beamwidth:

$$\text{ENBW} = \frac{\text{IPG}}{\text{CPG}} \quad (15)$$

Hamming weighting will be used in later examples with ENBW=1.36.

3.2 Random Phase Quantization Lobes

In the case of uncorrelated phase quantization error from element to element the analysis is particularly simple. The ratio of the desired response and the undesired response can be found from the expectation of the first and second terms of (13). The desired signal will be coherently added in the beamformer. The error component is assumed to be uncorrelated and will therefore be incoherently added. Although the phase quantization error in a sense is deterministic since it can be predicted from the quantization process, the case when the errors on individual channels are uncorrelated implies that one can consider the error to be a realization of a white, random process. That kind of phase quantization error will therefore be referred to as random. It has a uniform distribution over the quantization range $[-\pi/M_q, \pi/M_q]$, and a variance of $\pi^2/(3M_q^2)$. The resulting average voltage noise to signal ratio or sidelobe level is:

$$\text{SL}_{avg} = \frac{\left[\sum_{m=0}^{M-1} w_m^2 \right]^{1/2}}{\sum_{m=0}^{M-1} w_m} \sigma_{phase} = \frac{\pi}{M_q} \left(\frac{\text{ENBW}}{3M} \right)^{1/2} \quad (16)$$

This expression has been known for a long time in the radar literature [6].

The random error squared will be distributed according to a χ^2 distribution with 2 degrees of freedom (exponential distribution). The peaks of the squared error will therefore be a factor of 4.6 above the mean (1% percentile). The peak one-way sidelobe level (voltage) is therefore:

$$\text{SL}_{peak} \approx \frac{\pi}{M_q} \left(\frac{4.6 \cdot \text{ENBW}}{3M} \right)^{1/2} \quad (17)$$

An example of such a beampattern is shown in Fig. 1

3.3 Focusing quantization sidelobes in an unsteered system

In this case, the delay is given by (9) with $\theta = 0$. It is assumed that the Fresnel approximation is valid. The phase is:

$$\phi \approx 2\pi f \frac{[(m-M/2)d]^2}{2rc} = \pi u, u = \frac{[(m-M/2)d]^2}{r\lambda} \quad (18)$$

In the equation the phase has been expressed as a function of u . In that case the phase quantization error is a

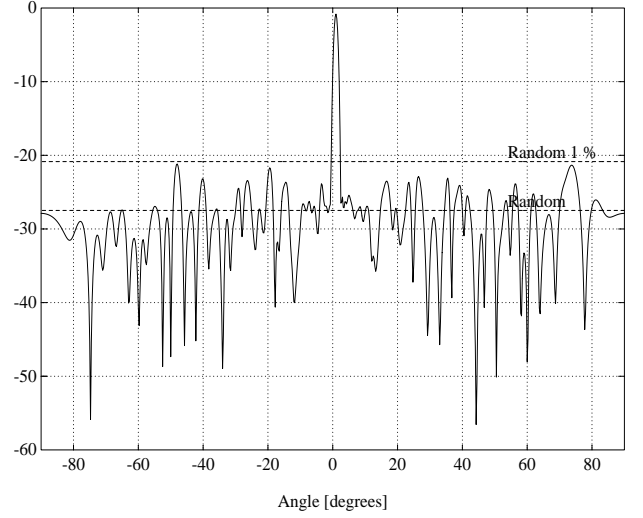


Fig. 1 Beampattern showing random sidelobes for a 5 MHz array with 128 elements. This is achieved by focusing to 20 mm and steering to 1 degrees and with quantization to 10 MHz.

sawtooth function and it can be expanded in the following Fourier series:

$$\exp(je(\phi)) = \sum_{k=-\infty}^{\infty} \frac{(-1)^k \sin(\pi/M_q)}{\pi(k+1/M_q)} \exp(jkM_q\phi) \quad (19)$$

It is seen that the phase of the functions in the expansion are themselves focusing functions. The interpretation of this equation is that the phase quantization error manifests itself as subsidiary foci at locations:

$$r_k = \frac{r}{kM_q}, k \neq 0 \quad (20)$$

Thus the response in the focal point is the sum of many defocused beams which all contribute to a raised sidelobe level [9].

In order to find the level of the sidelobes it is more instructive to look at the phase quantization error as a function of element number. Usually only the central part of the error is regular and is the main contributor to sidelobe peaks. Its extent can be found by equalling the phase from (18) with half the quantization step. The result is:

$$M_{central} = \frac{2M}{D} \left(\frac{r\lambda}{M_q} \right)^{1/2} \quad (21)$$

where r is the focused range and $D = Md$ is the aperture. To a first approximation this can be considered as one period of a cosine-shaped bulge over the central part of the array with amplitude π/M_q . The cosine is of period $2M_{central}$. The result is that there will be two spurious peaks offset by a wavenumber of $\pi/(M_{central}d)$ or

angles $\sin\theta = \pm\lambda/(2M_{central}d)$. The level of each peak can be found as in [8] and is given by the product of the correlation between a cosine and the actual central part of the quantization error, the quantization step-size and the fractional part of the aperture:

$$SL \approx \frac{1}{2} \frac{2}{\pi} \frac{\pi}{IPGM_q} \frac{M_{central}}{M} = \frac{M_{central}}{M_q \cdot M \cdot IPG} \quad (22)$$

There will also be additional peaks further away from the main lobe as shown in Fig. 2.

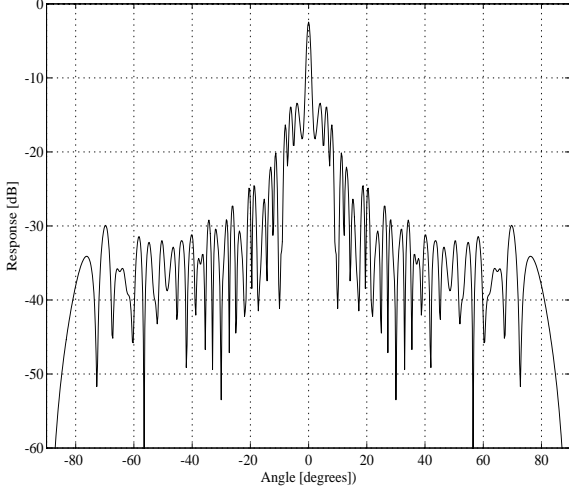


Fig. 2 Beampattern showing quantization sidelobes around the main lobe due to focusing for an unsteered 5 MHz array with 128 elements, focused to 90 mm and with quantization to 10 MHz.

3.4 Discrete quantization lobes in an unfocused system

The third effect of delay quantization is discrete quantization lobes that resemble grating lobes. In contrast to the previous point where the energy was defocused in depth, some of the energy is now used for undesired directions. This has been analyzed in the radar and sonar literature [6], [7], and occurs whenever the quantization error over the array becomes periodic. For an unfocused, uniform array, excited with CW, with element distance d , and a time delay quantization to accuracy $\tau_s = 1/f_s = 1/(M_q f_0)$, Gray [7] has given the condition for a periodic time delay quantization error over the array:

$$\left(p\tau_s = \frac{qd\sin\theta_{p,q}}{c} \right) \Rightarrow \sin\theta_{p,q} = \frac{p}{q} \frac{\lambda}{M_q d} \quad (23)$$

In comparing with (8) it is seen that this corresponds to the case when steering of a subarray of q elements gives a time delay which is an integral number, p , of delay

steps. The subarray is repeated periodically over the array when steered to direction $\theta_{p,q}$. There is a close relationship with grating lobes in linear arrays. The periodic quantization error gives rise to discrete sidelobes whose direction are given by the grating lobe direction in an array with element distance qd :

$$\sin\theta_k = k \frac{\lambda}{qd} + \sin\theta_{p,q} \quad k \in \{\dots, -2, -1, 1, 2, \dots\} \quad (24)$$

There is a very large number of combinations of p and q that will give valid angles, and therefore it is impossible to avoid discrete quantization lobes merely by avoiding to steer the array in certain directions. A closer analysis of the quantization lobes and their level is therefore necessary.

The worst-case quantization lobe is for $q=2$, where there will be $M/2$ periods of the quantization error.

The worst case is that every element will have a phase quantization error of $\pm\pi/(2M_q)$, i.e. plus or minus half the quantization step. The angles that give worst-case quantization lobe are $\theta_{1,2}$, $\theta_{3,2}$, $\theta_{5,2}$, etc.

The ratio of sidelobe to unquantized mainlobe level is the sum of the quantization error over the M/q subarrays relative to the coherent sum of the mainlobe, which for $q=2$ is:

$$SL_{q=2} = \frac{(M/2) \left(\sin \frac{\pi}{2M_q} + \sin \frac{\pi}{2M_q} \right)}{M} \approx \frac{\pi}{2M_q} \quad (25)$$

Fig. 3 gives an example of the beampattern obtained in this case.

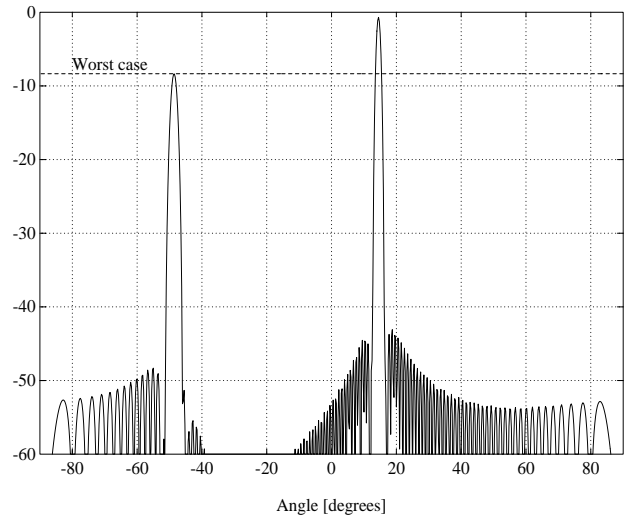


Fig. 3 Beampattern showing quantization sidelobes due to steering to 14.48 degrees ($p=1, q=2$) in the far-field for a 5 MHz array with 128 elements, and with quantization to 10 MHz.

There are three conditions that enhance this effect:

1. A regular array geometry, i.e. a uniform, non-curved linear or phased array
2. Continuous wave transmission
3. Far-field operation

The last condition is never satisfied in ultrasound imaging, and will help to decrease the quantization sidelobes in a medical ultrasound system in contrast to e.g. most sonar and radar systems. This leads to the last case, that of discrete sidelobes in combination with focusing.

3.5 Discrete Quantization Sidelobes and Focusing

In [8] expression (25) has been generalized to the case of a focused array. In that case only a subarray of length $M_{central} < M$, contributes to the periodic phase quantization error. $M_{central}$ is the same as was found in (21). When it is small compared to M , the worst-case discrete quantization lobe level is reduced by a factor:

$$SL_{red} \approx \frac{2M_{central}}{\pi} \frac{1}{M} \frac{1}{IPG} \quad (26)$$

Thus the sidelobe level becomes:

$$SL_{focus} \approx \frac{M_{central}}{M \cdot M_q} \frac{1}{IPG} \quad (27)$$

This is the worst-case sidelobe level in a beamformer which is focused. A beam plot that illustrates this case is shown in Fig. 4.

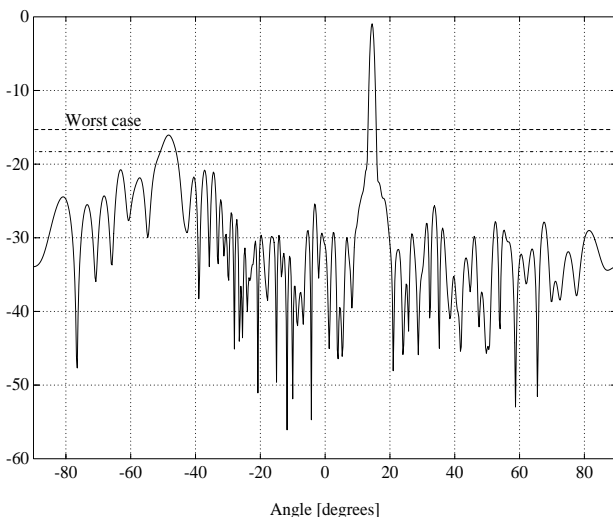


Fig. 4 Beam pattern showing quantization sidelobes due to a combination of steering and focusing. Conditions are as in Fig. 3 with the addition of focusing to 90 mm.

4. CONCLUSION

Several structures for realizing digital beamformers have been discussed. An analysis of quantization errors in a straight-forward implementation of a baseband beamformer has also been given. It has been shown how the sidelobe level due to phase quantization is affected by the time delay quantization step and by steering and focusing in the imaging system. A rule-of-thumb value for the time delay quantization step is that it should be in the order of the inverse of ten to twenty times the center frequency of the signal in order not to give noticeable effects.

It is expected that in the coming years digital beamformers will become a standard in medical ultrasound imaging systems due to their vastly improved capabilities for beam control, and for the possibility they offer for parallel receive beams.

5. REFERENCES

- [1] M. O'Donnell, W.E. Engeler, J.T. Pedicone, A.M. Itani, S.E. Noujaim, R.J. Dunki-Jacobs, W.M. Leue, C.L. Chalek, L.S. Smith, J.E. Piel, R.L. Harns, K.B. Welles and W.L. Hinrichs, "Real-time phased array imaging using digital beam forming and autonomous channel control," IEEE Ultrasonics Symposium, 1990, pp. 1499-1502.
- [2] S.H. Chang, S.B. Park, and G.H. Cho, "Phase-error free quadrature sampling technique in the ultrasonic B-scan imaging system and its application to the synthetic focusing system," IEEE Trans. Ultrason. Ferroelec., and Freq. Contr., vol 40, no 3, May 1993, pp 216-223.
- [3] D.P. Shattuck, M.D. Weinschenker, S.W. Smith, and O.T. von Ramm, "Explososcan: A parallel processing technique for high speed ultrasound imaging with linear phased arrays," J. Acoust. Soc. Am. vol. 75, no 4. April 1984.
- [4] R.G. Pridham and R.A. Mucci, "Digital interpolation beamforming for low-pass and bandpass signals," Proc. IEEE, Vol. 67, No. 6, June 1979.
- [5] B.D. Steinberg, "Digital beamforming in ultrasound," IEEE Trans. Ultrason. Ferroelec., and Freq. Contr., vol. 39, no 6, Nov. 1992.
- [6] T. C. Cheston, "Array antennas," chapter 11 in M. E. Skolnik (ed.), *Radar Handbook*, McGraw-Hill, New York, 1970.
- [7] D. A. Gray, "Effect of time-delay errors on the beam pattern of a linear array," IEEE Journ. Ocean. Eng., Vol. OE-10, No.3, July 1985.
- [8] S. Holm and K. Kristoffersen, "Worst-case analysis of phase quantization sidelobes in focused beamforming," IEEE Trans. Ultrason., Ferroelec. and Freq. Contr., vol. 39, Sept. 1992.
- [9] G. S. Kino, *Acoustic waves. Devices, Imaging, and Analog Signal Processing*, Prentice-Hall, 1987.